Scattering of light waves by electron electrostatic waves in laser produced plasmas*

Liu Zhan-Jun(刘占军)[a)b)†], Xiang Jiang(项 江)[b)], Zheng Chun-Yang (郑春阳)[a)b)],
Zhu Shao-Ping(朱少平)[b)], Cao Li-Hua(曹莉华)[b)],
He Xian-Tu(贺贤土)[a)b)], and Wang Yu-Gang(王宇钢)[a)]

[a)] *Center for Applied Physics and Technology, State Key Laboratory of Nuclear Physics and Technology, Peking University, Beijing* 100871, *China*

[b)] *Institute of Applied Physics and Computational Mathematics, Beijing* 100094, *China*

(Received 27 November 2009; revised manuscript received 6 January 2010)

The propagation of light waves in an underdense plasma is studied using one-dimensional Vlasov–Maxwell numerical simulation. It is found that the light waves can be scattered by electron plasma waves as well as other heavily and weakly damping electron wave modes, corresponding to stimulated Raman and Brilluoin-like scatterings. The stimulated electron acoustic wave scattering is also observed as a high scattering level. High frequency plasma wave scattering is also observed. These electron electrostatic wave modes are due to a non-thermal electron distribution produced by the wave–particle interactions. The collision effects on stimulated electron acoustic wave and the laser intensity effects on the scattering spectra are also investigated.

Keywords: scatterings, laser plasma, Vlasov simulation
PACC: 5225D, 5235, 5240D, 5265

1. Introduction

The stimulated Raman scattering (SRS),[1−4] a resonant decay of an incident light wave into a scattered light wave and an electron plasma wave (EPW), has been widely studied. Kinetic effects on the SRS have been investigated by particle-in-cell (PIC) simulation,[5,6] and by solving the Vlasov–Maxwell (VM) equations.[7−10] The electron acoustic wave (EAW) is normally heavily Landau damped but appears when the plasma electrons can be separated into hot and cold components, such as when there is stimulated excitation, when there is anomalous heating of electrons, or when electrons are trapped by large amplitude electrostatic waves or other structures.[11−13] EAW has dispersion relation $\omega = 1.31kv_{\rm te}$, where ω, k are the angular frequency and wavenumber, $v_{\rm te} = \sqrt{T_{\rm e}/m_{\rm e}}$ is the electron thermal velocity, $T_{\rm e}$ is the electron temperature and $m_{\rm e}$ is the electron mass. The interaction of light waves with the EAW has been observed experimentally.[14] In the experiment, the scattering level (the ratio of scattering energy to incident energy) is about 2×10^{-5}, and the EAW phase velocity is $1.4v_{\rm te}$. In the present paper, the excitation and scattering of electron electrostatic wave is investigated using the VM model. SRS is observed in the early stage of the propagation of the incident light wave. It is also found that the heavily and weakly damping electron electrostatic wave modes are also excited when a non-Maxwellian electron distribution is formed during the particle–wave interaction and the light wave can also be scattered by these wave modes. High phase velocity electron plasma wave and EAW scattering are also observed. The collision effects on EAW scattering and laser intensity effects on the scattering spectra are also investigated.

2. Physical model

The governing equations for the model[15] are the Krook equation[16] and Maxwell equations:

$$\partial_t f + v_x\partial_x f - \frac{e}{m_{\rm e}}\left(E_x + v_y B_z\right)\partial_{v_x} f = -\nu_{\rm ei}\left(f - f_0\right), \quad (1)$$

*Project supported by the National High-Tech ICF Committee of China, the National Natural Science Foundation of China (Grant Nos. 10975023, 10835003, 10935003 and 10974022) and the National Basic Research Program (Grant Nos. 2007CB815101, 2007CB814802 and 2010CB832904).
†Corresponding author. E-mail: liuzj@iapcm.ac.cn
© 2010 Chinese Physical Society and IOP Publishing Ltd

$$(\partial_t \pm c\partial_x) E^{\pm} = \frac{e}{\varepsilon_0} \int v_y f \mathrm{d}v_x, \tag{2}$$

$$E^{\pm} \equiv E_y \pm cB_z, \tag{3}$$

$$m_\mathrm{e} \partial_t v_y = -eE_y, \tag{4}$$

$$\partial_t E_x = \int v_x f \mathrm{d}v_x, \tag{5}$$

where f is the electron velocity distribution function (EVDF), ν_ei gives the electron–ion collision rate, f_0 is the initial equilibrium distribution function, c is the light speed in vacuum, E_x is the electrostatic field, E_y and B_z are the light electric and magnetic fields, respectively. v_y is the electron quiver velocity in laser field.

The light waves are linearly polarized in the y direction. The VM equations are solved by the operator splitting method. The space and velocity advections are performed using the third order van Leer method.[17] The boundary condition in x direction is periodic. We advance $E^{\pm}$ along their characteristics and specify $E^{\pm}$ at the boundary for the pump (or seed) light wave. To absorb the plasma waves generated by the backward SRS, ν_ei is taken to be large on the right side of the simulation box. Figure 1 shows the typical profiles of electron density and ν_ei in the simulation.

3. Simulation results

We now consider the scattering of an incident light wave by electron electrostatic waves. The incident light has wavelength $\lambda = 0.527$ μm and intensity $I = 1.6 \times 10^{16}$ W/cm^2, i.e., the normalized amplitude $a = eE_y/m_\mathrm{e}\omega_\mathrm{L}c$ is 0.057, where ω_L is incident light frequency. The total simulation length is $2000k_\mathrm{L}^{-1} \approx 168$ μm, where k_L is the incident wavenumber in vacuum. The plasma density is $0.03n_\mathrm{c}$, where n_c is the critical density, and located in the centre with two descending edges. The collision rate ν_ei is obtained by the formula[18] with ion charge 1 and Coulomb logarithm 8. We also set large ν_ei on the right part of the plasma to absorb the electrostatic waves when they travel to the plasma–vacuum interface. The configuration is also shown in Fig. 1. The initial electron velocity distribution function is Maxwellian with electron temperature 350 eV. The effect of ion motion has not been considered.

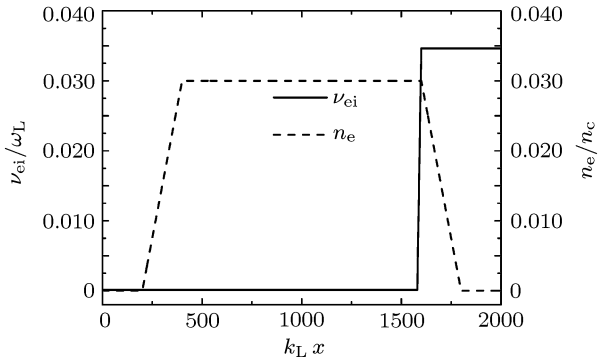


Fig. 1. The profiles of plasma density n_e and electron–ion collision rate ν_ei. The x-axis is normalized by the incident light wavenumber k_L in vacuum. The dashed line is the electron density profile, which normalized by the critical density n_c, and the solid line is the electron–ion collision rate, which normalized by the light angular frequency ω_L.

The time-integrated spectra of scattered light is shown in Fig. 2, where the x-axis is normalized by the incident light frequency and y-axis is in relative units. The incident light interacts with Maxwellian plasma, the stimulated Raman scattering can be first developed, as EPW is weakly damped. Other waves, such as EAW, is heavily damped. The EPW scattering is located $0.814\omega_\mathrm{L}$ under our physical parameters. According to the EPW dispersion relation $\omega^2 = \omega_\mathrm{pe}^2 + 3k^2v_\mathrm{te}^2$, the scattering light frequency should be $0.809\omega_\mathrm{L}$. However, it is noted that this EPW dispersion relation is not very exact for short waves[19] and large amplitude waves,[20] thus there is quite small difference between our simulation and analytical result. If the incident laser intensity is lower, the scattering light frequency is more near the theoretical results $0.809\omega_\mathrm{L}$. We also get the phase velocities of EPW is $3.99v_\mathrm{te}$, where $v_\mathrm{te} = 0.026c$ is the initial electron thermal velocity. The heavily damped EAW, which dispersion relation is $\omega = 1.31kv_\mathrm{te}$, can also scatter the light. Figure 2 shows that the frequency of scattering light by EAW is $0.932\omega_\mathrm{L}$, and the corresponding EAW phase velocity is $1.37v_\mathrm{te}$. The phase velocities of EPW and EAW are nearly with the experimental data. The amplitude of EAW in Fig. 2 is relative high and 0.06 times of that for EPW. Excepting the EPW and EAW scatterings, there are other wave modes scattering the light. The phase velocities of these electron electrostatic waves have values between $1.37v_\mathrm{te}$ and $5.48v_\mathrm{te}$. There are electron waves, which frequency is higher and/or lower than that of EPW, existing in the system. The scattering lights by these modes are even stronger than that of EPW. The scattering light frequency is varying with time. The formation of these changing waves is due to the EVDF changing during the wave—particle interactions.

The scattering light spectra in Fig. 2 is very broadly. Laser intensity has also influence the scatter-

ing spectra. We also plotted the scattering spectra for laser intensity 4×10^{15} W/cm^2 and 1×10^{15} W/cm^2 in the middle and bottom panels. For lower intensity laser light, the spectra width is less. For example, the scattering light spectra are between $0.805\omega_{\rm L}$ and $0.825\omega_{\rm L}$ for laser intensity 1×10^{15} W/cm^2 and between $0.800\omega_{\rm L}$ and $0.865\omega_{\rm L}$ for laser intensity 4×10^{15} W/cm^2. Some components of the scattering light spectra is less than $0.8\omega_{\rm L}$ for laser intensity 16×10^{15} W/cm^2. It means that there are electrostatic waves whose frequency is larger than that of EPW. While these spectra do not exist in lower incident light intensity cases, just as showed in the middle and bottom panels of Fig. 2.

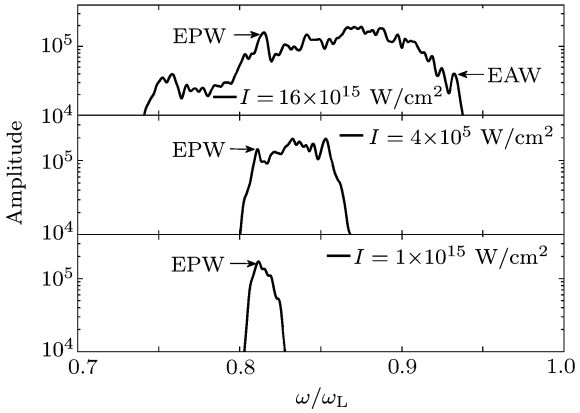


Fig. 2. The time-integrated spectra of reflected light with different incident lights. The x-axis is normalized by the incident light frequency $\omega_{\rm L}$ and y-axis is in relative units.

To explain these electrostatic modes, we show the electron distribution function at four different times in Fig. 3. It is found that high energy tails appear for $\omega_{\rm L}t = 10500$, 12000, 60000. Since the damping rate of electrostatic wave is proportional to the slope $\partial f/\partial v_x$, in some velocity intervals the slope

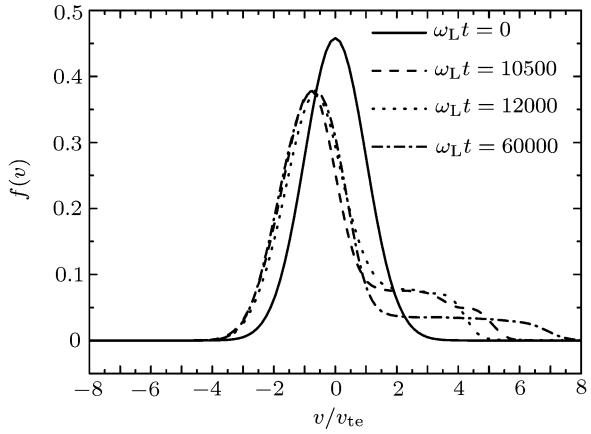


Fig. 3. The spatial averaged electron velocity distribution functions for four different times around $k_{\rm L}x = 725$.

is nearly zero. Thus the corresponding electrostatic waves can be developed. However, when EVDF is Maxwellian, these modes are heavily damped.

The dispersion relations of electrostatic wave can also be derived from the permittivity. The permittivity ε is define as

$$\varepsilon(\omega,k) = 1 - \frac{1}{k^2\lambda_d^2}\left[\mathcal{P}\int_{-\infty}^{\infty}\frac{\partial_{v_x}f(v_x)}{v_x-\omega/k}{\rm d}v_x + {\rm i}\,\pi\partial_{v_x}f(v_x)\right], \quad (6)$$

where ω and k are the frequency and wave vector of electrostatic waves, $\mathcal{P}$ represents the Cauchy principal value and $\lambda_{\rm d}$ is the Debye length. The roots of $\varepsilon = 0$ determine the weakly damping electrostatic modes which can exist in system. The real part of the permittivity based on the EVDF at $\omega_{\rm L}t = 12000$ in Fig. 3 is shown in Fig. 4. The black solid line shows the electrostatic wave modes which can scattering the incident light in backward. For $k\lambda_{\rm d} < 0$, there are only two wave branches. They are the usually EPW and EAW. But for $k\lambda_{\rm d} > 0$, there are four wave branches which all can scattering incident light. The EPW frequency in this case is $1.41\omega_{\rm pe}$, and its phase velocity $5.45v_{\rm te}$ is much higher than the thermal velocity. And it corresponds the scattering frequency $0.755\omega_{\rm L}$ in Fig. 2. Comparing with EVDF Maxwellian case, the EPW phase velocity is much higher for EVDF distortion.

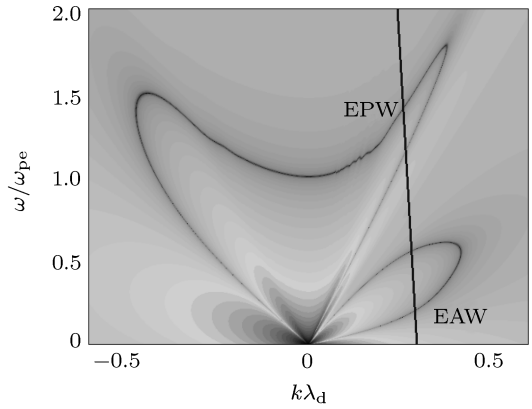


Fig. 4. The real part of the permittivity ε for the electrostatic waves, here the EVDF is same as Fig. 3 at $\omega_{\rm L}t = 12000$. The electrostic wave number is normalized by Debye length $\lambda_{\rm d}$, and the frequency is normalized by plasma frequency $\omega_{\rm pe}$. The gray line shows Re$\varepsilon = 0$. The black solid line shows the matched backward scattering electrostatic wave. Its intersection points with the gray lines have phase velocities $5.45v_{\rm te}$, $4.36v_{\rm te}$, $1.99v_{\rm te}$ and $0.70v_{\rm te}$.

The phase velocities of some electrostatic modes are in the plateau region of the EVDF (Fig. 4) or

much higher than the thermal velocity. These modes are weakly damped and can scatter the incident light, so the scattering spectra in Fig. 2 are broadly and even stronger than the EPW scattering. The phase velocities of other three branches that scattering light in backward are $4.36v_{\rm te}$, $1.99v_{\rm te}$ and $0.70v_{\rm te}$. While from Fig. 2, we obtain the electrostatic wave phase velocities are between $1.37v_{\rm te}$ and $5.45v_{\rm te}$. The EVDF in Fig. 3 at $4.36v_{\rm te}$ and $0.70v_{\rm te}$ has large slope, so the electrostatic dispersion relations in Fig. 4 have some errors. The EAW modes are heavily damped and normally cannot scatter light unless certain conditions are satisfied. The trapped particles and the modified EVDF can reduce the Landau damping, and EAW can be developed. While EAW is very easy damped by the collision effects. Taking the collision rate $\nu_{\rm ei}/\omega_L = 0, 0.64 \times 10^{-4}$, we found the scattering light spectra changing. The EAW scattering light amplitudes are 2.1 and 1.5 times larger than that with $\nu_{\rm ei}/\omega_L = 1.28 \times 10^{-4}$. For more heavily collision rate $\nu_{\rm ei}/\omega_L = 2.56 \times 10^{-4}$, we did not observed the stimulated EAW scattering, just as showed in Fig. 5. The collision rate can also affect other electrostatic waves. The scattering spectra amplitudes by modified Langmuir waves and other waves are stronger with large collision rate. Without collision effects, the EVDF is rapidly changing, the reflected spectra are broad and and low amplitudes. While with the weak collision effects, the EVDF is changing slowly, the scattering processes have some time to grow, the scattering spectra have large amplitude and narrow width. The spectra without collisions have some components near $\omega_{\rm L}$. But these scattering light disappeared with collisions.

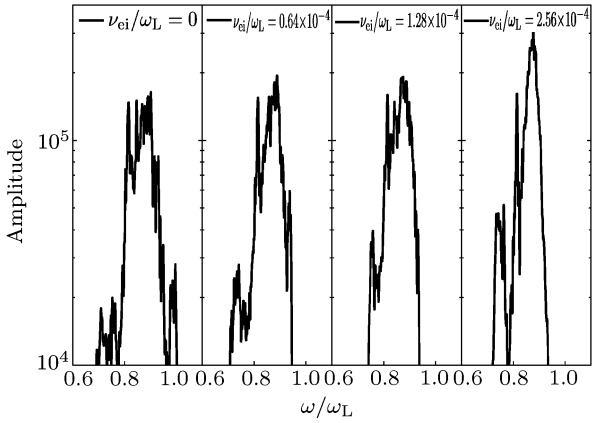


Fig. 5. The reflected light spectra for incident light intensity 1.6×10^{16} W/cm^2 with different collision rates.

4. Conclusion

In conclusion, we have shown that lots of electron electrostatic waves can be excited when an intense light beam propagates in a plasma because the EVDF is modified by the particle–wave interaction. It is found that the light waves can be scattered by electron plasma waves as well as other heavily and weakly damped electron acoustic modes, corresponding to stimulated Raman and Brilluoin-like scatterings. The stimulated electron acoustic wave scattering is also observed as a high level. Laser intensity and collision can both affect the EVDF during the interaction processes, the scattering spectra are also affected. The nonlinear frequency shift of Langmuir wave is red shift for electron trapping effects. Here we observed the blue shift of Langmuir wave for electron distribution function changed by nonlinear wave–particle interactions.

References

[1] Goldman M V and Dubois D F 1965 *Phys. Fluids* **8** 1404
[2] Baym G and Hellwarth R W 1965 *IEEE J. Quantum Electron.* **1** 309
[3] Liu C S, Rosenbluth M N and White R B 1974 *Phys. Fluids* **17** 1211
[4] Zhang L, Dong Q L, Zhao J, Wang S J, Sheng Z M, He M Q and Zhang J 2009 *Acta Phys. Sin.* **58** 1833 (in Chinese)
[5] Cao L H, Yu W, Xu H, Liu Z J, Zheng C Y and Li B 2004 *Chin. Phys.* **13** 1302
[6] Jin Z Y, Shen B F, Zhang X M, Wang F C and Ji L L 2009 *Chin. Phys.* B **18** 5395
[7] Califano F, Cecchi T and Chiuderi C 2002 *Phys. Plasmas* **9** 451
[8] Ghizzo A, Bertrand P, Shoucri M, Johnston T W, Fijalkow F and Feix M R 1990 *J. Comput. Phys.* **90** 431
[9] Liu Z J, Zhu S P, Cao L H and Zheng C Y 2007 *Acta Phys. Sin.* **56** 7084 (in Chinese)
[10] Liu Z J, Zhu S P, Cao L H, Zheng C Y, He X T and Wang Y G 2009 *Phys. Plasmas* **16** 112703
[11] Gary S P and Tokar R L 1985 *Phys. Fluids* **28** 2439
[12] Yu M Y and Luo H 2008 *Phys. Plasmas* **15** 024504
[13] Lu Q, Wang S and Dou X 2005 *Phys. Plasmas* **12** 072903
[14] Montgomery D S, Focia R J, Rose H A, Russell D A, Cobble J A, Fernández J C and Johnson R P 2001 *Phys. Rev. Lett.* **87** 155001
[15] Liu Z J, He X T, Zheng C Y and Wang Y G 2009 *Phys. Plasmas* **16** 093108
[16] Bhatnagar P L, Gross E P and Krook M 1954 *Phys. Rev.* **94** 511
[17] Mangeney A, Califano F, Cavazzoni C and Travnicek P 2002 *J. Comput. Phys.* **179** 495
[18] Kruer W L 1988 *The Physics of Laser Plasma Interactions* (Addison-Wesley Publishing Company) 55
[19] Liu Z J, Zheng J and Yu C X 2002 *Phys. Plasmas* **9** 1073
[20] Morales G J and O'Neil T M 1972 *Phys. Rev. Lett.* **28** 417